

Reentrance in the $\text{Mn}(\text{tetracyanoethylene})_x \cdot y(\text{CH}_2\text{Cl}_2)$ high- T_c molecule-based ferrimagnet

Charles M. Wynn and Mihai A. Gîrțu

Department of Physics, The Ohio State University, Columbus, Ohio 43210-1106

Jie Zhang and Joel S. Miller

Department of Chemistry, University of Utah, Salt Lake City, Utah 84112-0850

Arthur J. Epstein

Department of Physics and Department of Chemistry, The Ohio State University, Columbus, Ohio 43210-1106

(Received 15 October 1997; revised manuscript received 22 May 1998)

Results of static and dynamic magnetic studies of the compound $\text{Mn}(\text{TCNE})_x \cdot y(\text{CH}_2\text{Cl}_2)$ (TCNE = tetracyanoethylene) are reported. Curie-Weiss analysis of the high-temperature susceptibility data indicates a relatively strong exchange. The ac susceptibility, measured as a function of frequency and temperature, reveals frequency-independent peaks in both the in-phase and out-of-phase components of the susceptibility near 75 K. Additional peaks in both components, which are frequency dependent, are observed near 10 K. Weak irreversibilities, including a remanent moment and a bifurcation of the field-cooled (FC) and zero-field-cooled (ZFC) dc magnetizations are observed below 75 K. These irreversibilities become more pronounced below ~ 10 K. The presence of frequency dependence in the ac susceptibility and field dependence of the FC/ZFC magnetizations near 10 K but not at 75 K strongly suggest reentrance. Static scaling analysis at the high-temperature transition and dynamic scaling analysis at the low-temperature transition provide clear evidence for ordering with a spontaneous moment at 75 K and as a spin glass below 10 K. Possible mechanisms for this behavior are discussed. [S0163-1829(98)04937-6]

I. INTRODUCTION

Reentrance is an interesting phenomenon, most often observed in transition-metal-based alloys with spins residing in d orbitals, in which transitions from paramagnet to ferromagnet (FM) to spin glass (SG) are observed as temperature T is decreased. Counterintuitively, this implies that the FM phase has greater entropy than the SG phase. Current models¹ of the phenomena observed in "reentrant" magnetic materials suggest the observed behavior is not "true" reentrance, i.e., transition from pure paramagnet to pure FM to pure SG, but rather that a longitudinal FM order develops at higher T followed by a spin freezing of the individual transverse components at a lower T resulting in a magnet with randomly canted spins. A less accepted description¹ suggests that a percolating FM cluster occurs below the FM ordering temperature T_c which is broken up by the freezing of decoupled paramagnetic spins below the SG ordering temperature T_g . Recent studies of reentrance reveal many unexpected phenomena including a glassy "fragility" within the FM state.²

The initial discovery³ of a spontaneous moment at room temperature in the $\text{V}(\text{TCNE})_x \cdot y(\text{solvent})$ (TCNE = tetracyanoethylene) with spins in both p and d orbitals led to considerable interest in high- T_c molecule-based magnets and associated phenomena.⁴ Further work on $\text{V}(\text{TCNE})_x \cdot y(\text{CH}_3\text{CN})$ revealed interesting critical behavior, and a reentrant transition to a low-temperature SG state.⁵ Similarly, studies of $\text{V}(\text{TCNE})_x \cdot y(\text{C}_4\text{H}_8\text{O})$ suggest a transition from the magnetically ordered state to a state of noninteracting superparamagnetic particles at low temperature.⁶ The recent synthesis⁷ using the more air stable Mn ion in place of the V ion, results in $\text{Mn}(\text{TCNE})_x \cdot y(\text{CH}_2\text{Cl}_2)$. This

compound is an electron transfer salt with unpaired spins on both the transition metal ion and the bridging organic molecule. The results of a study of the precursor of the magnet $\text{Mn}^{\text{II}}[\text{C}_4(\text{CN})_8](\text{CH}_3\text{CN})_2 \cdot (\text{CH}_2\text{Cl}_2)$, and the similarities with $\text{Fe}(\text{TCNE})_2 \cdot y(\text{CH}_2\text{Cl}_2)$, a compound from the same family, for which Mössbauer spectroscopy studies indicated a state of oxidation of 2, suggest that Mn is present as $S = 5/2$ Mn^{II} implying the formula $\text{Mn}^{\text{II}}(\text{TCNE})_2 \cdot y(\text{CH}_2\text{Cl}_2)$.⁷ The cyanocarbon acceptor $[\text{TCNE}]^-$ has a spin of $1/2$ due to an unpaired electron in a molecular orbital of π^* character. Unlike the reentrant $\text{V}(\text{TCNE})_x \cdot y(\text{solvent})$, for which the structural correlation length is short and depends upon the solvent used (e.g., ~ 10 , 15 , and 25 Å, when the solvent is CH_3CN , $\text{C}_4\text{H}_8\text{O}$, and CH_2Cl_2 , respectively^{5,6}), the $\text{Mn}(\text{TCNE})_2 \cdot y(\text{CH}_2\text{Cl}_2)$ diffraction pattern exhibits sharp x-ray diffraction lines⁷ indicating a much less disordered structure.

We present here results of magnetic studies of $\text{Mn}(\text{TCNE})_2 \cdot y(\text{CH}_2\text{Cl}_2)$, which strongly support reentrant behavior in this molecule-based magnet with spins in both p and d orbitals. While the frequency (f) dependence of the ac susceptibility and the field dependence of the field-cooled (FC) and zero-field-cooled (ZFC) magnetizations suggest traditional reentrant phenomena, the evolution of the system from ferrimagnet to SG reveals intriguing phenomena including an increase in the magnetization upon cooling into the SG state. The experimental results are compared to current models of reentrance. The outline of this paper is as follows. In Sec. II, we discuss the experimental apparatus and techniques. In Sec. III we report the results of ac susceptibility and dc magnetization studies, together with static and dynamic scaling analyses at the two transitions, respectively.

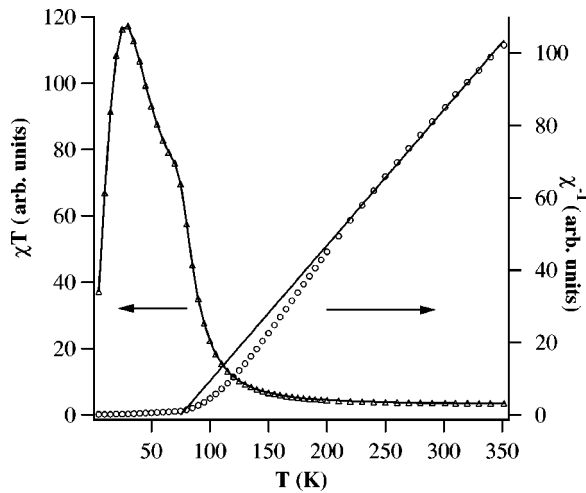


FIG. 1. χT (left axis) and χ^{-1} (right axis) as functions of T , measured in dc applied fields of 100 Oe. The solid line is a fit to the Curie-Weiss law for $230 \leq T \leq 350$ K.

Section IV consists of a discussion of these data stressing the two transitions in the context of a reentrant ferrimagnetic system. Section V summarizes our conclusions.

II. EXPERIMENT

The preparation of the samples is described elsewhere.⁷ Magnetization M data were collected using a Quantum Design MPMS-5 superconducting quantum interference device magnetometer with a continuous-flow cryostat and a 5.5 T superconducting solenoid. Susceptibility data at various f (5–10 000 Hz) were recorded on a Lake Shore 7225 ac susceptometer/dc magnetometer with an exchange cryostat and 5.0 T superconducting solenoid. Additional data at 1 kHz and various ac amplitudes (1–10 Oe) were collected near 75 K to increase the signal-to-noise response. Calibration of the absolute magnitude of the susceptibility along with determination of the proper phases of the instrument were made using a $\text{HgCo}(\text{SCN})_4$ paramagnetic material. All magnetic data were taken on polycrystalline samples that had been sealed under argon in quartz EPR tubes to avoid degradation with air. Studies on multiple samples from more than ten batches reproducibly show similar overall behavior with minor variations of less than 1 K for the high- T and $\sim \pm 2$ K for the low- T transition, attributed to the variation of solvent content from sample to sample. The molar susceptibilities for the data reported here were calculated using $x \sim 0.8$ solvent, based on elemental and thermogravimetric analyses.⁷

III. RESULTS AND ANALYSIS

The dc susceptibility χ_{dc} (the ratio of magnetization M to field H) from 5–350 K at $H=100$ Oe is displayed as χT and $1/\chi$ versus T in Fig. 1. The χT product increases as T is lowered from 350 K, with a shoulder near 80 K and a larger peak near 20 K. A value of $\theta=76$ K was obtained from a fit of the $1/\chi$ curve above 230 K to the Curie-Weiss law, $\chi \propto (T-\theta)^{-1}$. As orbital momentum is quenched in a Mn(II) system and the accompanying second-order zero-field splitting effects are expected to be small,⁸ the large θ value indi-

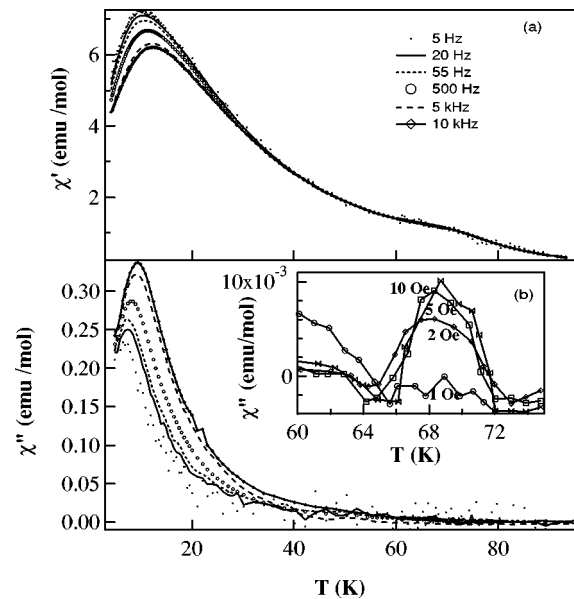


FIG. 2. (a) χ' and (b) χ'' as functions of T , measured in $H_{\text{ac}}=1$ Oe at various frequencies (legend). Inset shows χ'' as a function of T , measured at 1 kHz in various H_{ac} (see labels).

cates a relatively large exchange. We note, however, that the positive Curie-Weiss θ also could be due to fitting for $T \leq 4\theta$, where the mean field behavior is not necessarily applicable. Higher- T data may lead to negative θ , indicating ferrimagnetic behavior.⁹

The in-phase χ' and out-of-phase χ'' components of the complex ac susceptibility as a function of f (5–10000 Hz) and T (5–100 K) are shown in Figs. 2(a) and 2(b). χ' displays a small frequency-independent shoulder at 75 K and a larger frequency-dependent peak near 10 K. The onset of an obvious frequency dependence in χ' occurs near 30 K, though the frequency dependence in χ'' is observable as high as 60 K. A frequency-dependent peak in χ'' is observed near 10 K, however, no obvious feature is observed near 75 K. In an effort to improve the signal to noise ratio at 75 K, the susceptibility was measured at 1 kHz in various ac amplitudes (1–10 Oe) near 75 K [inset Fig. 2(b)], revealing a small peak in χ'' centered at ~ 69 K.

The magnetization was measured in various H (5–200 Oe) by cooling in zero field from 100 to 5 K, applying a field, and collecting data while warming to 100 K (ZFC), then collecting data in the field while cooling from 100 to 5 K (FC), Fig. 3. The FC data were independent of whether the data were collected while warming or cooling. A small *field-independent* bifurcation of the FC and ZFC curves is observed near ~ 72 K. These irreversibilities become more pronounced near ~ 10 K, at which temperature a *field-dependent* peak is observed in the ZFC curves. The temperature of the peak in the ZFC curves decreases as H increases, changing from 11 K in 5 Oe to 6 K in 200 Oe.

Remanent magnetization was measured to probe the formation of a spontaneous moment. The compound was cooled in 50 Oe from 100 to 5 K at which point the longitudinal field was zeroed to within ± 0.02 Oe (a nonzero transverse field is expected from the uncompensated transverse component of the Earth's field). The remanent magnetization was measured while warming from 5 to 90 K, Fig. 4. The rema-

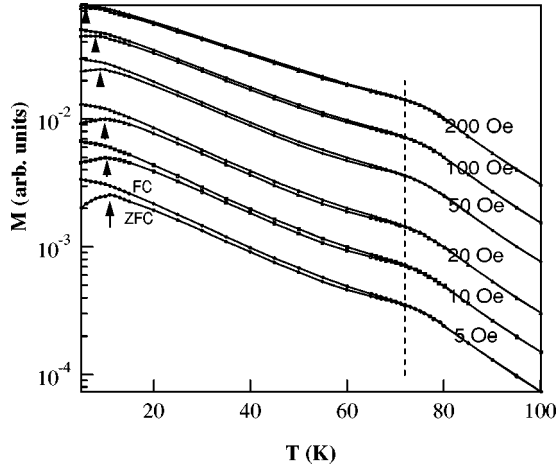


FIG. 3. FC (upper curves) and ZFC (lower curves) magnetizations as functions of T in various applied fields (see labels). Lines and arrows are guides to the eye.

nence decreases sharply from 5 to 20 K after which it decreases gradually until it disappears at 75 K.

The low- T isothermal hysteresis curves obtained by zero-field cooling and measuring in fields of up to 55 kOe display an increase in coercive fields (H_c) as T decreases, Fig. 5, with $H_c < 5$ Oe at 35 K and $H_c \sim 50$ Oe at 2 K. Isothermal data $M(H)$, Fig. 6, were collected for various T (69–89 K) by zero-field cooling and measuring from 0 to 55 kOe, for scaling analysis near 75 K.

In systems with the spontaneous magnetization as order parameter, the traditional approach to scaling¹¹ is to measure $M(H, T)$ near T_c and attempt to collapse the data onto two universal curves (corresponding to data above and below T_c) by plotting $M/|t|^\beta$ versus $H/(M|t|^{\beta\delta})$ where $t = (T - T_c)/T_c$, and β and δ are critical exponents defined by

$$M \sim t^\beta, \quad (1)$$

$$M \sim H^{1/\delta}. \quad (2)$$

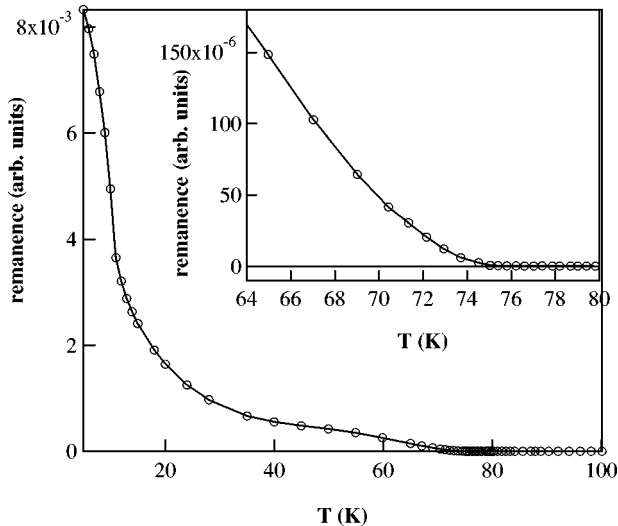


FIG. 4. Remanent magnetization as a function of T obtained by cooling in 50 Oe from 100 to 5 K, zeroing the field at 5 K to within ± 0.02 Oe, and measuring on warming in zero applied field.

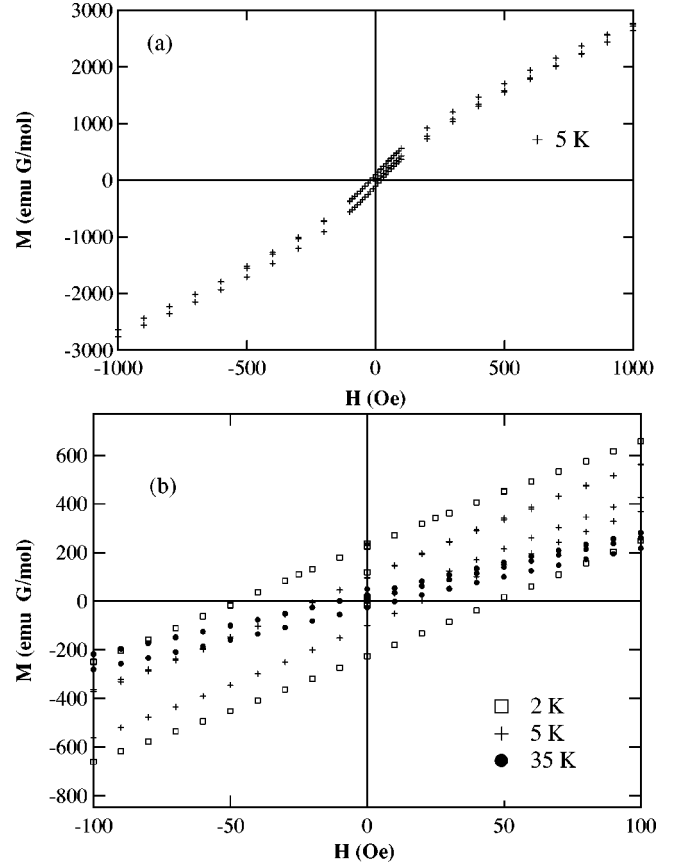


FIG. 5. $M(H)$ hysteresis curves at (a) 5 K and (b) 2, 5, 35 K.

A successful data collapse involves the ‘‘best’’ choice of three parameters β , δ , and T_c . To minimize the number of free parameters, we fix T_c at 75 K as determined independently from the remanence (Fig. 4). We then use the $M(H)$ curve at T_c along with Eq. (2) to obtain δ . The log-log fit at 75 K (inset Fig. 6) for $H > 2$ T yields $\delta = 3.86$. We thus fix $\delta = 3.86$ and also choose 2 T as the lower bound for data to be used in our scaling analysis. It is noted that, in general, H must be large enough to remove domain wall effects yet still small relative to T .¹¹ The scaling analysis is now performed with β as the only free parameter. Figure 7(a) shows the best data collapse using a traditional scaling plot with $\beta = 0.35$ (similar to the value of 0.36 expected for a three-dimensional Heisenberg system¹⁰). The traditional scaling plot, however, displayed using logarithmic axes, may hide deviations from scaling. Thus we also display our data using an alternate scaling function¹¹ that allows linear axes, Fig. 7(b). The range of reduced temperature $|t|$ is 0.005 to 0.18.

Noting the behavior of $\chi''(\omega, T)$ near 10 K, the applicability of a dynamic scaling analysis in which q_{EA} , the Edwards-Anderson (EA) order parameter, is expected to diverge, was investigated. Similar to static scaling, dynamic scaling involves the collapse of the data onto a universal curve via the choice of the ‘‘best’’ exponents and T_g . The relevant exponents $z\nu$ and β_g are defined near T_g , the SG transition temperature,¹²

$$\tau \sim |t_g|^{-z\nu}, \quad (3)$$

$$q_{EA} \sim t_g^{-\beta_g}, \quad (4)$$

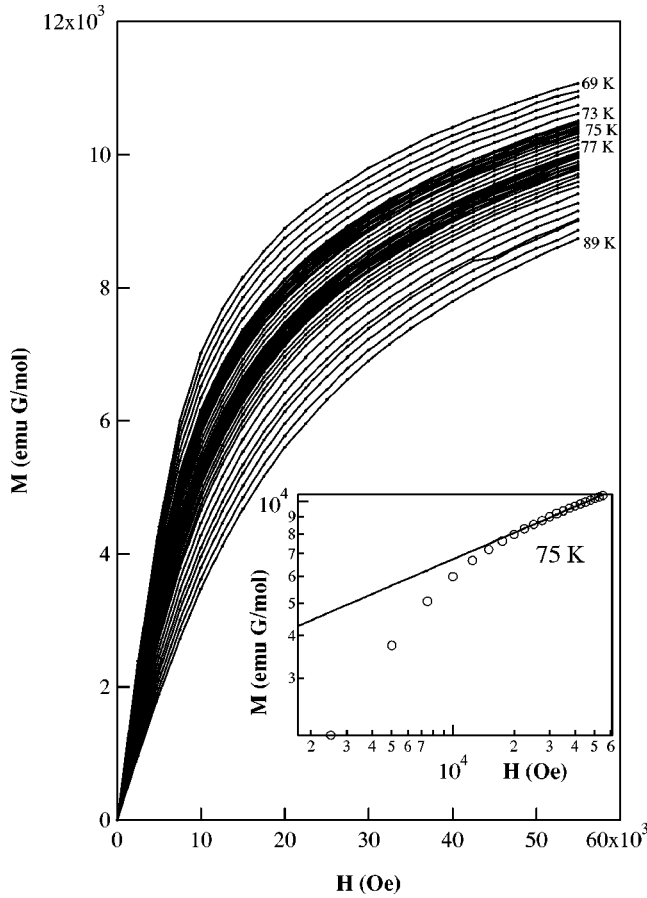


FIG. 6. $M(H)$ as measured at various T ranging from 69 to 89 K. The inset shows $M(H)$ at 75 K on logarithmic axes. The solid line is a fit of the high field M to a power law in H .

with τ the spin relaxation time, and $t_g = (T - T_g)/T_g$. It is noted that T_g and β_g are related to the divergence of the q_{EA} order parameter in a manner analogous to T_c and β , which describe the behavior of the spontaneous moment as FM order parameter.

Following the technique proposed by Geschwind *et al.*¹³ to analyze $\chi''(\omega, T)$ data near T_g [Fig. 8(a)], $\chi''T/\omega\beta_g^{1/z\nu}$ is plotted versus $t_g/\omega^{1/z\nu}$ with β_g , $z\nu$, and T_g varied to obtain the best collapse of the data onto a universal curve. Unlike traditional dynamic scaling plots, this plot allows the use of linear axes, which more clearly show deviations from good scaling. The ratio $\beta_g/z\nu$ was determined prior to scaling by noting that the peaks of $\chi''T$ should behave as $\chi''_p(\omega)T_p(\omega) \sim \omega\beta_g^{1/z\nu}$. The linear fit to the log-log plot of $\chi''_p(\omega)T_p(\omega)$ versus ω [Fig. 8(b), inset] yields a value of $\beta_g/z\nu = 0.086$. This value was held fixed and a best collapse of the dynamic data (for $T < 20$ K) was obtained [Fig. 8(b)] using $T_g = 2.5$ K, $\beta_g = 1.7$, and $z\nu = 20$. The data collapse reasonably well over the three decades in frequency, with the expected increase in deviations for larger t_g (farther from T_g and the critical region).

IV. DISCUSSION

We first discuss the absence or presence of frequency dependence as indicative of the nature of the two transitions. The typical relaxational processes in a system with sponta-

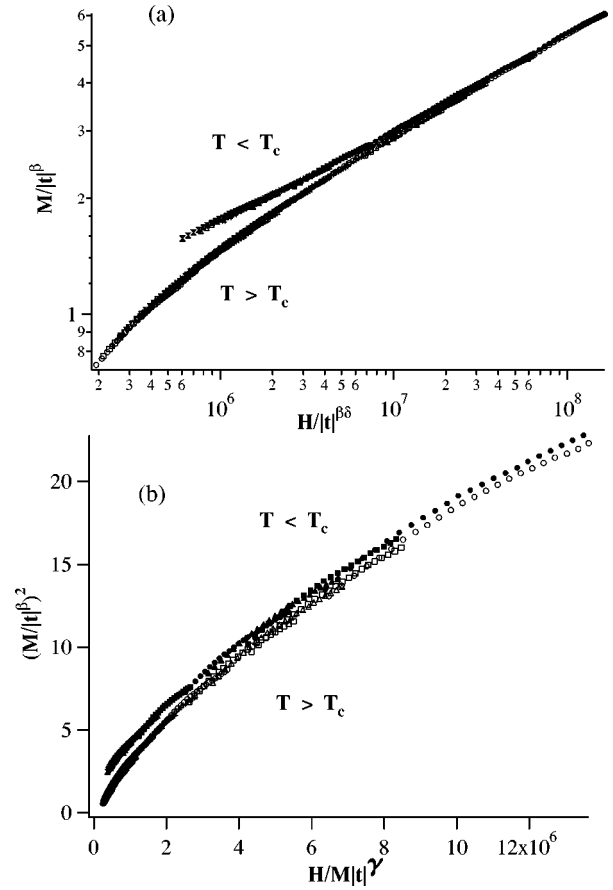


FIG. 7. Static scaling analyses using $H \geq 2$ T data from Fig. 5. T_c was fixed at 75 K based on determination from remanence data (Fig. 4) and $\delta = 3.86$ based on $M(T_c) \sim H^{1/\delta}$ (Fig. 6). β was varied to obtain the best collapse of the data, resulting in $\beta = 0.35$. (a) $M/|t|^\beta$ vs $H/|t|^{\beta\delta}$ on logarithmic axes, (b) $(M/|t|^\beta)^2$ vs $H/(M|t|^\gamma)$ on linear axes.

neous moment are fast enough ($\tau \sim 10^{-11}$ s) that the system is expected to equilibrate over macroscopic distances in a time much shorter than our experimental timescales of $\sim 10^0 - 10^{-4}$ s, even considering the critical slowing down occurring near T_c .¹⁴ Thus, it is generally expected^{12,15} that, unlike glasses, there will be no frequency dependence over the frequency range commonly used in ac susceptibility experiments for a ferromagnetic or ferrimagnetic system. For ferromagnets the pinning of the domain walls causes frequency dependence of the microwave frequency susceptibility, the few cases in which such f dependence is seen in ac susceptibility measurements being primarily related to the mobility of pinning centers in systems with annealed disorder.^{16,17} As we expect quenched disorder in our system, we take the absence of frequency dependence of the ac susceptibility near 75 K as evidence that this transition is to a nonglassy state with a spontaneous moment. In contrast, a SG is characterized by long relaxation times and is expected to exhibit frequency dependence of the ac susceptibility.^{12,15}

Based on the ac susceptibility data we propose that at about 75 K there is a transition to a phase with a spontaneous moment (likely ferrimagnetic, as discussed below) while below 10 K the system has a spin glasslike behavior. (T_g is always below the lowest frequency peak temperature because it is defined in the dc limit of the ac data.)

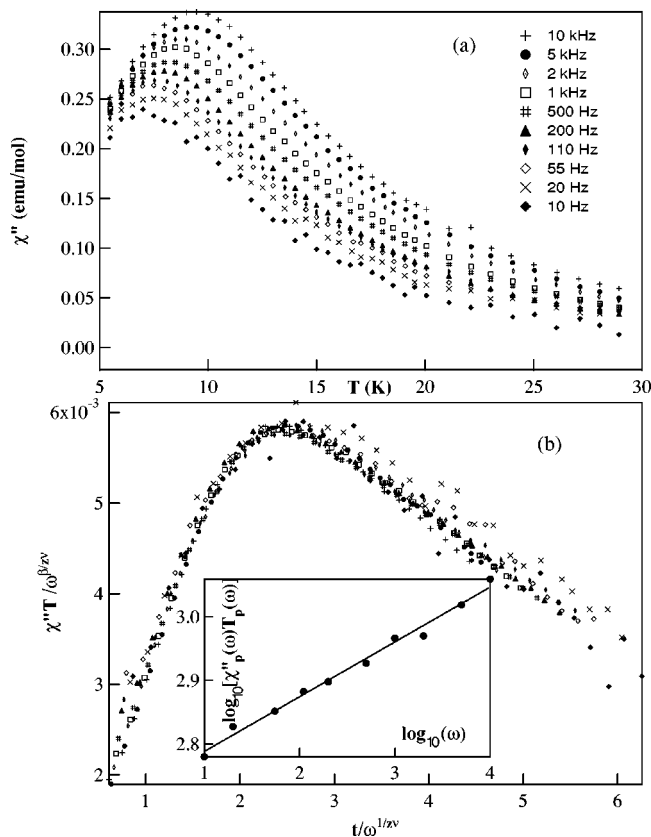


FIG. 8. (a) $\chi''(T)$ at various frequencies (legend). (b) Dynamic scaling analysis based on the data in (a) below 20 K. Inset shows a plot of the peak values $\log_{10}[\chi''_p(\omega)T_p(\omega)]$ vs $\log_{10}(\omega)$ over three decades in frequency with the slope yielding a value of $\beta_g/z\nu = 0.086$. This ratio was held fixed while β_g , $z\nu$, and T_g were varied to obtain the best collapse of the data, which gave $T_g = 2.5$ K, $\beta_g = 1.7$, and $z\nu = 20$.

Since frequency dependence may also occur in systems other than spin glasses (such as superparamagnets), we quantify the frequency dependence as the relative variation of the peak temperature T_p per decade of frequency $(\Delta T_p/T_p)/[\Delta(\log_{10} f)]$. This gives a value of 0.078 for $\text{Mn}(\text{TCNE})_2 \cdot \gamma(\text{CH}_2\text{Cl}_2)$, at the upper limit of the typical range of values observed in traditional spin glasses, which range from 0.004 to 0.08, and not very different from the well-studied reentrant system EuSrS .¹² The successful scaling analysis is further evidence of a SG transition. The values of β_g and $z\nu$ are, however, somewhat larger than those obtained for more traditional SG systems,¹⁸ highlighting the unusual nature of this molecule-based compound. Higher values of $z\nu$ and lower values of T_g are obtained when one attempts to get better data collapse at low temperatures.¹⁸

$\text{Mn}(\text{TCNE})_2 \cdot \gamma(\text{CH}_2\text{Cl}_2)$ shows increased irreversibilities in the FC/ZFC magnetizations near 10 K. These increased or “strong” irreversibilities, in addition to the long relaxation times, are expected on approaching the SG state from either the FM or paramagnetic state.^{19,20} The strong irreversibilities near 10 K are in contrast with the relatively weak irreversibilities near 75 K. The field dependence of the FC/ZFC bifurcation temperatures near 10 K also contrasts the absence of field dependence near 75 K. A decrease in the bifurcation temperature with increasing H , as observed near 10 K, is

expected near the freezing line associated with a SG transition.²¹

Thus the experimental results and analysis strongly suggest reentrance, i.e., transition to a state with a spontaneous moment at 75 K and transition to a SG state at 2.5 K. In particular the appearance of a spontaneous moment at 75 K is supported by the buildup of a bulk magnetic moment evidenced by the increase in χT with decreasing temperature (Fig. 1), the shoulder in χ' near 75 K (Fig. 2), the hysteresis implied by the peak in χ'' ,²² near 75 K (Fig. 2), the onset of field-independent irreversibilities in the FC/ZFC curves near 75 K (Fig. 3), the appearance of a remanent moment near 75 K (Fig. 4), and a successful scaling analysis of the isothermal magnetization data near 75 K (Figs. 6 and 7). Characteristic SG behavior near or below 10 K was evidenced by the appearance of frequency-dependent ac susceptibility cusps along with a strong absorptive term near 10 K (Fig. 2), the onset of field-dependent irreversibilities (Fig. 3) near 10 K, an increase in H_c near 10 K (Fig. 5) expected near a SG transition,²³ and a successful dynamic scaling analysis (Fig. 8).

Other reentrant systems have been identified showing similar behavior. Of note is the $(\text{Fe}_{0.90}\text{Cr}_{0.05}\text{Ni}_{0.05})_2\text{P}$ system, which also shows frequency independence of χ at the FM transition and frequency dependence at the SG transition.²⁴ The observation of reentrance in $\text{V}(\text{TCNE})_x \cdot \gamma(\text{solvent})$ and $\text{Mn}(\text{TCNE})_2 \cdot \gamma(\text{CH}_2\text{Cl}_2)$ (both p and d -orbital based magnets) suggests a generality of the phenomenon for this class of materials. In the parent compound $\text{V}(\text{TCNE})_x \cdot \gamma(\text{solvent})$, however, this behavior was attributed to randomness in the anisotropy due to random dilution of the $[\text{TCNE}]^-$ by the nonmagnetic solvent CH_3CN .⁵ In contrast to the $\text{V}(\text{TCNE})_x \cdot \gamma(\text{solvent})$, in which the x-ray scattering data revealed only short-range structural order (of order 10–25 Å), powder x-ray data of the $\text{Mn}(\text{TCNE})_2 \cdot \gamma(\text{CH}_2\text{Cl}_2)$ show relatively sharp lines (presence of structural correlation lengths ≥ 100 Å), similar to the results reported for $\text{Fe}(\text{TCNE})_2 \cdot \gamma(\text{CH}_2\text{Cl}_2)$.⁷ Furthermore, the isothermal magnetization curves of $\text{Mn}(\text{TCNE})_2 \cdot \gamma(\text{CH}_2\text{Cl}_2)$ are significantly different from those of the $\text{V}(\text{TCNE})_x \cdot \gamma(\text{solvent})$ and, unlike $\text{V}(\text{TCNE})_x \cdot \gamma(\text{solvent})$, do not conform to random anisotropy predictions. Also, as orbital momentum is quenched in a Mn^{II} system and any accompanying second-order effects are expected to be small,⁸ the single-ion anisotropy is less likely to play as major role as in the V compound. The reentrant behavior for $\text{Mn}(\text{TCNE})_2 \cdot \gamma(\text{CH}_2\text{Cl}_2)$ is more likely related to the presence of random frustration. Thus, while both compounds show reentrance, there are significant differences.

Experimental studies of the exchange between Mn^{III} porphyrin donors and $[\text{TCNE}]^-$ acceptors in the crystalline quasi-one-dimensional manganoporphyrin systems have shown strong antiferromagnetic (AF) coupling²⁵ as expected from a system with large overlap of spin-carrying orbitals in which kinetic exchange dominates. Similarly, the coupling between Mn^{II} ($S = 5/2$) and TCNE ($S = 1/2$) in the present compound is expected to be AF, which would imply that the spontaneous moment is due to ferrimagnetic ordering. Thus the positive Curie-Weiss temperature θ is likely due to the limited temperature range at high T . Data at

higher T should show a change in the slope of the $1/\chi$ curve, leading to negative θ .

The increase of the magnetic moment with decreasing T below the FM transition is unusual for a reentrant system, the current models of reentrance mentioned in the Introduction, predicting an evolution from FM to SG accompanied by either a constant or decreasing magnetization. However, these models describe systems with only single magnitude spins in contrast to the presence of two spin values in $\text{Mn}(\text{TCNE})_2 \cdot y(\text{CH}_2\text{Cl}_2)$.

Noticing that glassines and the increase of the magnetic moment seem to occur simultaneously, we are led to speculate that there may be a connection between ferrimagnetism and the formation of the glassy state. Given the crystallinity of these compounds it is likely that a magnetic lattice exists within each crystallite and it consists of various sublattices, (made up of Mn, and TCNE's, respectively). The magnetic moment could increase, while decreasing the temperature, due to the difference between the exchange coupling between the various sublattices and the different temperature variation of the sublattice moments, as was previously shown for ferrites.²⁶ The various exchange interactions between sublattices may lead to canted spin configurations²⁷ while competing interactions may occur mostly at low temperatures due to the differences between those sublattices.

The ability of the TCNE molecule to bind in different orientations (at the same crystal sites) may contribute to disorder and glassiness in this system, similar to the previously studied manganese-porphyrin compounds.²⁸ The small structural disorder likely caused by solvent vacancies and various orientations of the TCNE bridging molecule may be more significant at low temperatures, where the spins realign in

different configurations, in order to minimize the free energy. Disorder and frustration may then cause the glassy behavior found in this compound.

V. CONCLUSION

$\text{Mn}(\text{TCNE})_2 \cdot y(\text{CH}_2\text{Cl}_2)$ exhibits strong exchange and a relatively high transition temperature ($T_c = 75$ K). The appearance of a remanent magnetization χ'' and the onset of field-independent bifurcations in the FC/ZFC magnetizations at or near 75 K indicate a spontaneous moment likely due to a ferrimagnetic transition. Below ~ 10 K, a crossover to a SG-like state ($T_g = 2.5$ K) is evidenced by the onset of frequency-dependent maxima in the ac susceptibility in addition to enhanced field-dependent irreversibilities in the FC/ZFC magnetizations. Successful scaling analyses near both transitions indicates that two phase transitions are occurring. We speculate that the unusual increase of the magnetic moment toward the SG transition may be due to ferrimagnetism and the presence of various sublattices with different exchange coupling and different temperature dependences of the sublattice magnetizations. We further speculate that at low temperature there may be a competition between the various interactions among sublattices, which together with the slight structural disorder may contribute to the unusual behavior observed in this system.

ACKNOWLEDGMENTS

We wish to acknowledge the assistance and discussion with D. G. Gordon and support provided in part by the U.S. DOE under Grant Nos. DE-FG02-86BR45271, DE-FG03-93ER45504, and DE-FG02-96ER12198.

-
- ¹M. J. P. Gingras, in *Magnetic Systems with Competing Interactions*, edited by H. T. Diep (World Scientific, Singapore, 1994).
- ²K. Jonason, J. Mattsson, and P. Nordblad, *Phys. Rev. Lett.* **77**, 2562 (1996).
- ³J. M. Manriquez, G. T. Yee, R. S. Mclean, A. J. Epstein, and J. S. Miller, *Science* **252**, 1415 (1991).
- ⁴S. Ferlay, T. Mallah, R. Ouahes, P. Veillet, and M. Verdaguer, *Nature (London)* **378**, 701 (1995); T. Malleah, S. Thiebaut, M. Verdaguer, and P. Veillet, *Science* **262**, 1554 (1993).
- ⁵P. Zhou, B. G. Morin, J. S. Miller, and A. J. Epstein, *Phys. Rev. B* **48**, 1325 (1993).
- ⁶P. Zhou, S. M. Long, J. S. Miller, and A. J. Epstein, *Phys. Lett. A* **181**, 71 (1993).
- ⁷J. Zhang, J. Ensling, V. Ksenofontov, P. Gutlich, A. J. Epstein, and J. S. Miller, *Angew. Chem. Int. Ed. Engl.* **37**, 657 (1998); J. Zhang, L. M. Liable-Sands, A. L. Rheingold, R. E. Del Sesto, D. G. Gordon, B. M. Burkhardt, and J. S. Miller, *J. Chem. Soc. Chem. Commun.* **1998**, 1385.
- ⁸A. Abragam and B. Bleaney, *Electron Paramagnetic Resonance of Transition Ions* (Dover, New York, 1986).
- ⁹The assumed composition of $x=2$, $y=0.8$ (molecular weight of 373.5 g/mol) yields a high-temperature χT product (~ 3 emu K/mol at 350 K) less than the Curie constant of 5.2 emu K/mol expected for a spin 5/2 and two spins 1/2. This may be due to differing values of x and/or y which would affect the molar susceptibility and magnetization values [similar anomalies were observed in the $\text{V}(\text{TCNE})_x \cdot y(\text{solvent})$; see A. J. Epstein and J. S. Miller, *Mol. Cryst. Liq. Cryst.* **228**, 99 (1993)], larger Mn oxidation reducing the $S=5/2$ spin value, or the experimental limitations preventing us from collecting data at temperatures higher than 350 K.
- ¹⁰P. M. Chaikin and T. C. Lubensky, *Principles of Condensed Matter Physics* (Cambridge University Press, Cambridge, 1995), p. 231.
- ¹¹S. N. Kaul, *J. Magn. Magn. Mater.* **53**, 5 (1985).
- ¹²J. A. Mydosh, *Spin Glasses: An Experimental Introduction* (Taylor and Francis, London, 1993).
- ¹³S. Geschwind, D. A. Huse, and G. E. Devlin, *J. Appl. Phys.* **67**, 5249 (1990).
- ¹⁴D. S. Fisher, G. M. Grinstein, and A. Khurana, *Phys. Today* **41** (12), 56 (1988).
- ¹⁵K. H. Fischer and J. A. Hertz, *Spin Glasses* (Cambridge University Press, New York, 1991), p. 267.
- ¹⁶G. H. J. Wentenaar, S. J. Campbell, D. H. Chaplin, K. R. Sydney, and G. V. H. Wilson, *Phys. Rev. Lett.* **37**, 1767 (1976).
- ¹⁷S. Chikazumi, *Physics of Magnetism* (Wiley, New York, 1966), Chap. 15; R. M. Bozorth, *Ferromagnetism* (Van Nostrand, New York, 1951), p. 788.
- ¹⁸S. Geschwind, D. A. Huse, and G. E. Devlin, *Phys. Rev. B* **41**, 4854 (1990); L. P. Levy, *ibid.* **38**, 4963 (1988).
- ¹⁹I. Mirebeau, S. Itoh, S. Mitsuda, T. Watanabe, Y. Endoh, M.

- Hennion, and R. Papoular, *Phys. Rev. B* **41**, 11 405 (1990).
- ²⁰W. Abdul-Razzaq and J. S. Kouvel, *Phys. Rev. B* **35**, 1764 (1987).
- ²¹D. S. Fisher and D. A. Huse, *Phys. Rev. B* **38**, 386 (1988); C. M. Soukoulis, K. Levin, and G. S. Grest, *Phys. Rev. Lett.* **48**, 1756 (1982).
- ²²F. Palacio, F. J. Lazaro, and A. J. Van Duyneveldt, *Mol. Cryst. Liq. Cryst.* **176**, 289 (1989).
- ²³S. Senoussi, *J. Phys. (Paris)* **45**, 315 (1984).
- ²⁴B. K. Srivastava, A. Krishnamurthy, V. Ghose, J. Mattsson, and P. Nordblad, *J. Magn. Magn. Mater.* **132**, 124 (1994).
- ²⁵C. M. Wynn, M. A. Gîrțu, J. S. Miller, and A. J. Epstein, *Phys. Rev. B* **56**, 315 (1997); **56**, 14 050 (1997); C. M. Wynn, M. A. Gîrțu, K-I. Sugiura, E. J. Brandon, J. L. Manson, J. S. Miller, and A. J. Epstein, *Synth. Met.* **85**, 1695 (1997); C. M. Wynn, M. A. Gîrțu, W. B. Brinckerhoff, K-I. Sugiura, J. S. Miller, and A. J. Epstein, *Chem. Mater.* **9**, 2156 (1997).
- ²⁶E. W. Gorter, *Philips Res. Rep.* **9**, 295 (1954); **9**, 321 (1954); **9**, 403 (1954).
- ²⁷Y. Yafet and C. Kittel, *Phys. Rev.* **87**, 290 (1952).
- ²⁸M. A. Gîrțu, C. M. Wynn, K. I. Sugiura, J. S. Miller, and A. J. Epstein, *J. Appl. Phys.* **81**, 4410 (1997); *Synth. Met.* **85**, 1703 (1997).